Accepted Manuscript

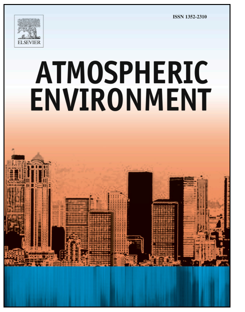

Effects of moisture content on wind erosion thresholds of biochar

F.C. Silva, C. Borrego, J.J. Keizer, J.H. Amorim, F.G.A. Verheijen

PII: S1352-2310(15)30487-8

DOI: 10.1016/j.atmosenv.2015.10.070

Reference: AEA 14228

To appear in: *Atmospheric Environment*

Received Date: 30 April 2015

Revised Date: 23 October 2015

Accepted Date: 26 October 2015

Please cite this article as: Silva, F.C., Borrego, C., Keizer, J.J., Amorim, J.H., Verheijen, F.G.A., Effects of moisture content on wind erosion thresholds of biochar, *Atmospheric Environment* (2015), doi: 10.1016/j.atmosenv.2015.10.070.

This is a PDF file of an unedited manuscript that has been accepted for publication. As a service to our customers we are providing this early version of the manuscript. The manuscript will undergo copyediting, typesetting, and review of the resulting proof before it is published in its final form. Please note that during the production process errors may be discovered which could affect the content, and all legal disclaimers that apply to the journal pertain.

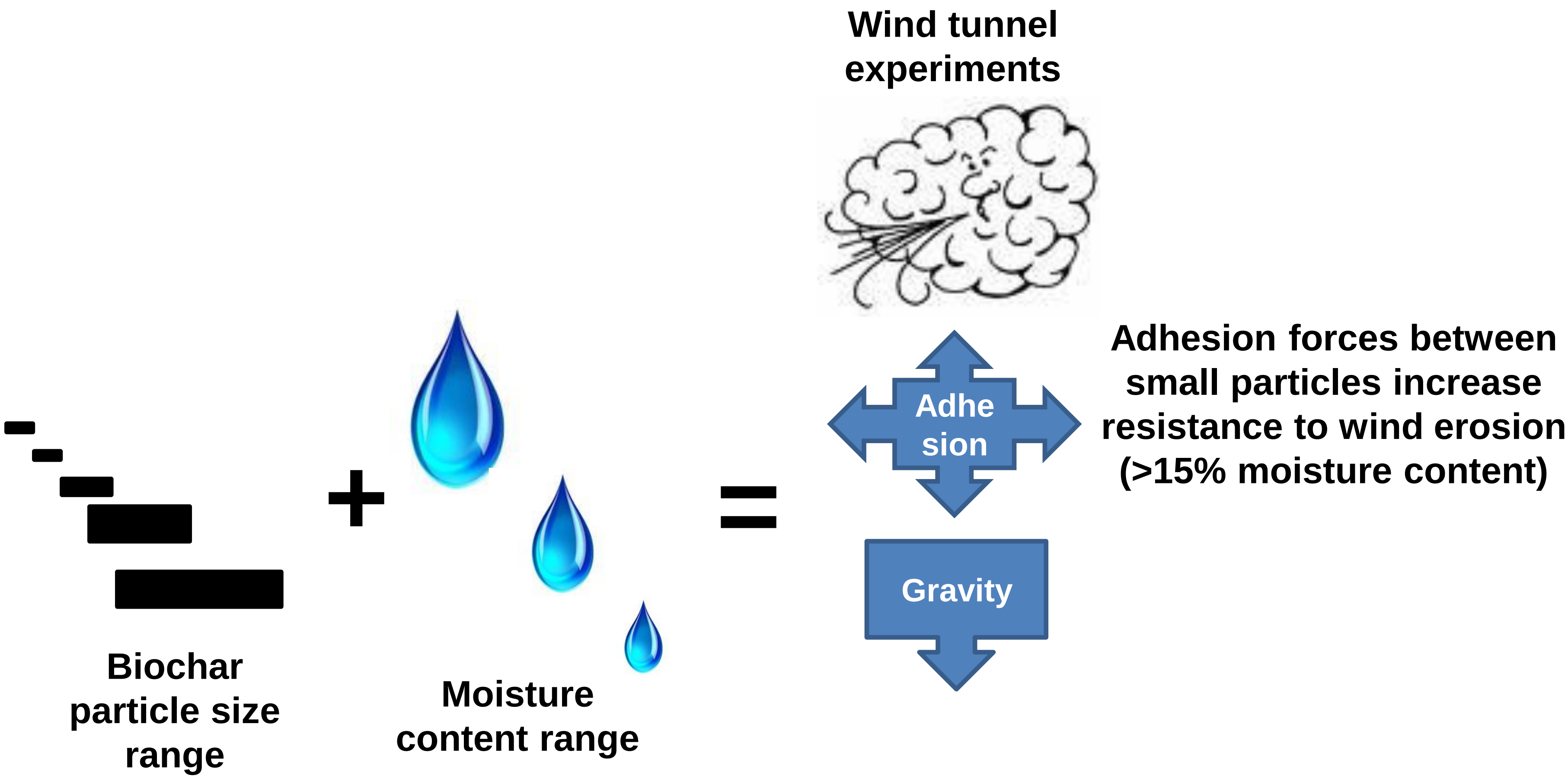
Wind tunnel experiments
Adhe sion
Gravity
Adhesion forces between small particles increase resistance to wind erosion (>15% moisture content)
Biochar particle size range
Moisture content range

ACCEPTED MANUSCRIPT

Effects of moisture content on wind erosion thresholds of biochar

F.C. Silva[1], C. Borrego[1], J.J. Keizer[1], J.H. Amorim[1,2], F.G.A. Verheijen[1,]*

[1]University of Aveiro, Centre for Environmental and Marine Studies (CESAM), Department of Environment and Planning, Campus Santiago, 3810-193 Aveiro, Portugal

[2]Swedish Meteorological and Hydrological Institute (SMHI), Air quality research unit, SE-60176 Norrköping, Sweden

*Corresponding author: frankverheijen@gmail.com, Tel.: +351 234 370 200

Highlights

- Wind erosion of biochar was assessed through wind tunnel simulations
- Moisture content lower than 10 % does not prevent erosion of fine particles
- Higher moisture increases adhesion of fine particles and weight of large particles
- Minimum 15 % moisture is recommended for reducing wind erosion of biochar

Abstract

Biochar, i.e. pyrolysed biomass, as a soil conditioner is gaining increasing attention in research and industry, with guidelines and certifications being developed for biochar production, storage and handling, as well as for application to soils. Adding water to biochar aims to reduce its susceptibility to become air-borne during and after the application to soils, thereby preventing, amongst others, human health issues from inhalation. The Bagnold model has previously been modified to explain the threshold friction velocity of coal particles at different moisture contents, by adding an adhesive effect. However, it is unknown if this model also works for biochar particles. We measured the threshold friction velocities of a range of biochar particles (woody feedstock) under a range of moisture contents by using a wind tunnel, and tested the performance of the modified Bagnold model. Results showed that the threshold friction velocity can be significantly increased by keeping the gravimetric moisture content at or above 15 % or greater to promote adhesive effects between the small particles. For the specific biochar of this study, the modified Bagnold model accurately estimated threshold friction velocities of biochar particles up to moisture contents of 10 %.

Keywords

biochar; threshold friction velocity; wind tunnel; particle size; Bagnold model

ACCEPTED MANUSCRIPT

Abbreviations

ρ	Density
β	Adhesive effect parameter
A	Aerodynamic constant
a	Conceptual contribution of gravity to threshold friction velocity
B	Regression coefficients of the response surface methodology
b	Conceptual contribution of adhesive forces to threshold friction velocity
d_m	Mean particle size diameter
dP	Pressure differential
k	von Kármán constant
RSM	Response surface methodology
U	Free stream velocity
*U**	Threshold friction (or shear) velocity
W	Gravimetric water content
Z	Height

1. Introduction

Airborne dust particles have raised concerns for both environmental (Choobari et al., 2014; IPCC, 2013) and human health reasons (De Capitani et al., 2007; Hashizume et al., 2010; Karanasiou et al., 2012; Salvi and Barnes, 2009). Known sources of dust aerosols, including black carbon, range from biomass and fossil fuel burning (Andreae and Merlet, 2001; Ito and Penner, 2005; Jacobson, 2001), wind erosion of aggregate storage piles of coal and charcoal (Toraño et al., 2007), to rail and road transport, including through re-suspension (Buchsbaum, 2007; Ferreira et al., 2003; Harrison et al., 2012)

The concept of biochar, where biomass is pyrolised to create a char that can improve soil functioning (Lehmann, 2007), has received increasing scientific attention in the last years (Verheijen et al., 2014). The main research focus has been on soil carbon sequestration (Lehmann et al., 2006; Nguyen and Lehmann, 2009) and crop yields (Jeffery et al., 2011), but biochar has also been observed to change many other soil processes and functions (Lehmann and Joseph, 2015). The pyrolysis process can cause carbonaceous dust emissions, although pyrolysis generally produces substantially less black carbon aerosols than biomass burning (Whitman et al., 2011). Nonetheless, biochar particles can also become air-borne after the pyrolysis process, namely: i) during post-processing, packing, storage and transport; ii) during application in the field; and iii) through soil erosion by wind during the lifetime of biochar in soil. Considering the post-production process, the European Biochar Certificate recommends that biochar should be kept “sufficiently moist to prevent dust generation or dust explosions”, but does not quantify the relevant moisture contents (Schmidt et al., 2012). At the start of writing this paper, a search of the SCOPUS database for “biochar and wind” only retrieved one relevant article, i.e. a paper about applying biochar below the soil surface to avoid the risk of erosion by wind (Blackwell et al., 2010). Verheijen et al. (2010) also stated that there is a paucity of data on interactions between biochar and wind to inform sustainable biochar development.

Relationships between moisture content and threshold friction velocities have been observed for coal dust (Duo-min and Shu-tang, 1991) and have also been modelled for a range of coal particle sizes by means of the modified Bagnold model (Zhang et al., 2012; 2013). However, biochar has different physical properties than coal and it is unknown if the model developed for coal particles is also valid for biochar particles. The objectives of this study were, therefore: i) to determine the relationships between moisture content and threshold friction velocity for the full range of particles (<50 µm to >6,000 µm) of a common, woody feedstock biochar; ii) to test if the contribution of adhesive and gravity forces can be predicted by the modified Bagnold model; and iii) to discuss the implications of our findings for biochar production and application. To this end, we conducted wind erosion experiments in the wind tunnel of the Department of Environment and Planning (University of Aveiro) to determine threshold velocities for biochar particles of 6 size classes and at 6 moisture contents.

2. Materials and methods

2.1. Biochar source and preparation

Biochar was purchased from Swiss-Biochar GmbH, where it was produced from a mixed wood sievings feedstock in a Pyreg® 500 III pyrolysis unit, 620 °C maximum temperature, 20 min duration, 80 % C content and H/C ratio 0.18. The main physico-chemical characteristics are presented in Table 1. Six particle size classes were obtained by mechanical sieving at 5000, 3150, 2000, 200 and 50 µm mesh widths. The resulting particle size classes are identified according to their mean particle size as shown in Table 2, where the largest particle size class was assumed to have a mean of 6,000 µm. Subsequently, the biochar fractions were oven-dried at 75 ^{0}C for 48 h.

The different biochar particle size classes were combined with six contents of gravimetric moisture to achieve a full-factorial experiment of two factors and six levels per factor, with 3 to 5 replicates for each of the 36 combinations. The gravimetric water contents (1, 3, 6, 10, 15 and 20 %) were selected to cover a similar range as used in other studies on the influence of moisture content on particle transport by wind (Chen et al., 1996; Zhang et al., 2012).

The moisture contents were attained by calculating the required mass of water, assuming that the density of distilled water is approximately 1 kg L^{-1}, and verified by measuring weight loss following heating at 105 ºC for 24 h. Specific volumes of biochar were put into plastic bags and then wetted with a liquid dispenser (atomizer) producing a fine spray (Cornelis and Gabriels, 2003; Han et al., 2009). The plastic bags were then placed in a refrigerator at 4 ^{0}C for a minimum period of 24 h to achieve homogeneous wetting of the biochar.

ACCEPTED MANUSCRIPT

Table 1. Bulk biochar physico-chemical characteristics.

Characteristic	**Value (average ± standard deviation)**
Electrical conductivity of the leachate (µS cm^{-1})	1,496 ± 43
pH	8.13 ± 0.04
pH of the leachate	9.96 ± 0.07
Ash content (%)	10.36 ± 0.97
Density (kg m^{-3})	184 ± 4

2.2. Wind tunnel experiments

2.2.1. Experimental setup

The experimental work was performed in the wind tunnel laboratory facilities of the Department of Environment and Planning, at the University of Aveiro, Portugal. These facilities consist of an open-circuit, suction type wind tunnel, with a test section of 7×1.5×1 m (length × width × height), as described in (Borrego et al., 2007).

Biochar samples were placed over a white surface (for maximizing colour contrast) that was centred on the test section floor of the wind tunnel. A square of 36 cm^2 was filled with sample material up to a height of approximately 0.5 cm (Figure 1). During the actual wind tunnel experiments, three moments were defined for visual observation and recording of the pressure differential (*dP*): (i) moment 1, when sample particles started to vibrate, corresponding to the threshold shear stress; (ii) moment 2, when particles from the sample edges started to be transported, representing the incipient motion; and (iii) moment 3, when particles from the sample centre started to be transported, representing the major contribution of the entrainment (Dey, 1999). More specifically, moments 2 and 3 were defined as when five particles had been eroded. As in several other wind tunnel soil erosion experiments (e.g., Alfaro et al., 1997; Dong et al., 2003; He et al., 2008; Genis et al., 2013), a Pitot tube was used for the measurement of wind velocity, mainly due to its robustness when working with particle-fed flows. Free stream velocity ranged from 0.63 to 10.28 m s^{-1}, with a rotor frequency-step between consecutive measurements of 2.5 Hz (corresponding to an average velocity-step of 0.54 m s^{-1}).The vertical wind profile was determined by measuring *dP* at 12 heights (*Z*) from the wind tunnel floor, ranging from 0.5 to 50.0 cm (the latter corresponding to half the height of the wind tunnel). Free stream wind velocity ranged from 0.0 to 10.3 m s^{-1}.

ACCEPTED MANUSCRIPT

Figure 1. Biochar sample on wind tunnel test section floor.

2.2.2. Experimental determination of threshold friction velocity

The vertical wind velocity profile in the atmospheric boundary layer under neutral stability conditions can be described by the logarithmic relation:

$$U(Z) = \left(\frac{U^*}{k}\right) ln\left(\frac{Z}{Z_0}\right) \qquad (1)$$

, where U is the free stream velocity, U^* is the threshold friction velocity, k is the von Kármán constant (0.4), and Z_0 is the aerodynamic roughness height.

Eq. (1) may be approximated by a least-squares curve fitting method (Dong et al., 2003), which, then, enables the determination of U^*, if the variation of velocity with height is known. This method was applied, using the values for the velocity determined by the Pitot tube and the respective height, and is represented by:

$$U(Z) = M \cdot ln(Z) + N \qquad (2)$$

, where M and N are regression constants.

The threshold friction velocity is obtained by:

$$U^* = k \times M \qquad (3)$$

2.2.3. Statistical analysis

The analysis of variance (two-way ANOVA with interaction model) was applied to the U^* values of moment 3 (particles detaching from the centre of the sample, see Section 2.2.1), as these are the most representative of field conditions. This analysis was used to test significance of particle size and moisture content, as well as their interaction, on threshold friction velocities, and it was performed in the software package IBM SPSS™ version 20.

Furthermore, the response surface methodology (RSM) was also applied in order to better illustrate the combined influence of particle size and moisture content. This methodology was only applied to the $U*$ values of moment 3, as these are the most representative of field conditions. The experimental results were modelled according to Eq. (4):

$$U*_{mod} = B_0 + B_1 x_1 + B_2 x_2 + B_{1,2} x_1 x_2 + B_{1,1} x_1^2 + B_{2,2} x_2^2 \qquad (4)$$

, where $U*_{mod}$ is the response variable, x_1 represents the gravimetric water content (W, in %), x_2 represents the mean size of each class of biochar particles (d_m, in μm), B_0 is the model constant, B_1 and B_2 are linear coefficients (main effects), $B_{1,2}$ is a cross-product coefficient (interaction) and $B_{1,1}$ and $B_{2,2}$ are quadratic coefficients (Myers et al., 2009). Fitting was done with the software package Matlab™ version R2011b, using the least squares method. To this end, the ranges of both factors (W and d_m) were codified (x_1 and x_2) between -1 and 1, as shown in Table 2 The goodness-of-fit was assessed by R^2 as well as the significance of the regression model (F-test).

Table 2. Codification of the gravimetric water content (x_1) and the mean size of each class of biochar particles (x_2), for application of the response surface methodology.

***W* (%)**	1	3	6	10	15	20
x_1 (codified)	-1	-0.789	-0.473	-0.053	0.474	1
d_m (μm)	6,000	4,075	2,575	1,100	125	40
x_2 (codified)	1	0.354	-0.149	-0.644	-0.971	-1

2.3. Modelling of the threshold friction velocity

Modelling of $U*$, like their statistical analysis, was done just for the experimental data of moment 3. For each particle size class, $U*$ was modelled as a linear function of W, following Eq.(5):

$$U* = bW + a \qquad (5)$$

, where b and a represent the contributions of the adhesive forces between particles and of gravity, respectively. This linear relationship allows assessing which of these two forces are dominant in the threshold friction velocity for a given particle size class (Zhang et al., 2012).

Aeolian transport of particles can furthermore be modelled as a function of the aerodynamic drag force that lifts the particles, taking into account particle size and density as well as air density. This is usually done assuming that the aerodynamic related constant (A) has a value around 0.10 (Bagnold, 1941). The original Bagnold model, however, did not explicitly consider the effect of the particles' water content. Therefore, Zhang et al. (2012) recently proposed to introduce the effect of the water content, in particular for modelling the Aeolian transport of coal particles transported by wind. This modified Bagnold's model is defined as Eq. (6):

$$U^* = A\sqrt{\frac{1}{1-W}}\sqrt{\frac{\rho_{biochar}}{\rho_{air}}g.d_m} \quad (6)$$

, where $\rho_{biochar}$ and ρ_{air} are the densities of biochar and air, respectively, and g is the acceleration of gravity. While the A in the modified Bagnold model needs to be determined experimentally, the model can be further extended to determine the contribution of the adhesive forces by adding a term (β) that is defined as a power law function of both gravimetric water content and mean particle diameter:

$$\beta = \frac{W^c}{{d_m}^d} \quad (7)$$

, where c and d are non-negative parameters.

The extended model then becomes Eq. (8):

$$U^* = A\sqrt{\frac{1}{1-W}}\sqrt{\frac{W^c}{{d_m}^d}}\sqrt{\frac{\rho_{biochar}}{\rho_{air}}g.d_m} \quad (8)$$

3. Results

Although the data set is slightly non-linearly distributed (p-value = 0.050 for Kolmogorov-Smirnov test), error's variances are equal (p-value = 0.049 for Levene test). Therefore, two-way analysis of variance was performed, and showed that each of the studied factors (d_m and W), as well as their interaction on U^*, were all significant at a significance level of 0.05 (Table S1 provided as supplementary material). These results anticipated that the effect of particle size on threshold friction velocity is more pronounced than moisture or even than the interaction between both factors. Subsequent results are, therefore, presented by focusing on the effect of each separated factor on threshold friction velocity of biochar particles.

3.1. Effect of particle size

The observed U^* values for moments 1 and 2 (when the particles started to vibrate and to be eroded from the sample edges, respectively) are given as supplementary material, in Figures S1 and S2 respectively.

The U^* values for moment 1 could not be measured for the two smaller particle size classes (d_m of 40 and 125 µm), as indicated by the zero values in Figure S1. The observed U^* values for moment 1 ranged from 0.17 m s^{-1} (d_m = 1,100 µm with W = 10%) to 0.33 m s^{-1} (d_m = 4,075 µm with W = 20%). This wide range can be attributed primarily to the heterogeneity in the size of the biochar particles. These differences in particle size may have been associated to differences in other relevant factors such as the particles' aerodynamic behaviour, shape sphericity, tortuosity, ratio between length and thickness (platyness *sensu* (Boton et al., 2013)), pore size distribution, mechanical strength, orientation, and density (including packing fraction). The U^* values for moment 1 revealed a clear tendency to increase with increasing particle size (at least up to 4,075 μm), regardless of the particles' moisture content. This increase in U^* values was most pronounced between particle sizes 2,575 to 4,075 μm, especially for the higher moisture contents (6 – 20 %). In contrast, U^* values hardly changed or even decreased between particle sizes 4,075 μm to 6,000 μm, possibly because the smaller particles were more platy than the larger ones, as observed by (Terzaghi, 1996), and, thus, experienced a stronger shear stress.

The U^* values for moment 2, (Figure S2), showed a similar behaviour as moment 1: generally, U^* increased with increasing particle size, up to a d_m of 4,075 μm. Moment 2 U^* values ranged from 0.15 to 0.49 m s^{-1}, for d_m = 125 μm at W = 6 % and d_m = 4,075 μm at W = 15 %, respectively. Edge erosion may not represent field-scale applications of biochar in soil. All the centre particle erosion events (moment 3) presented higher U^* values. In this study, centre particles eroding are seen as a more representative assessment of the field-scale reality and are analysed in more detail below.

The U^* values for the moment 3, (Figure 2) ranged from 0.25 m s^{-1} (d_m = 125 μm at W = 1 %) to 0.61 m s^{-1} (d_m = 6,000 μm at W = 20 %). U^* values increased with increasing particle size class (except for d_m = 6,000 μm at W = 3 % and W = 10 %). The most obvious pattern was that U^* tended to be higher for smaller particle size classes (d_m of 40 and 125 μm) when moisture contents were greater than 1 %. For d_m of 40 and 125 μm particle size classes, 3 % and 10 % moisture contents resulted in U^* values between 0.27 and 0.30 m s^{-1}, very similar to those obtained for larger particles with d_m = 1,100 μm (U^* between 0.29 and 0.30 m s^{-1}). Further increases in moisture content (15 % and 20 %) resulted in significant (p-value < 0.001) U^* increases for the small particle size classes (0.38 – 0.39 m s^{-1} and 0.41 – 0.43 m s^{-1} for d_m of 40 and 125 μm, respectively). This observation is in accordance with (Zhang et al., 2012), who found that the moisture content had considerably greater impacts on U^* of smaller than larger coal particles. These authors reported that below d_m = 250 μm, and above W = 6 %, U^* was not particle size dependent but rather dependent on moisture content, which they attributed to the weight-moisture gain and inter-particle aggregation.

ACCEPTED MANUSCRIPT

ACCEPTED MANUSCRIPT

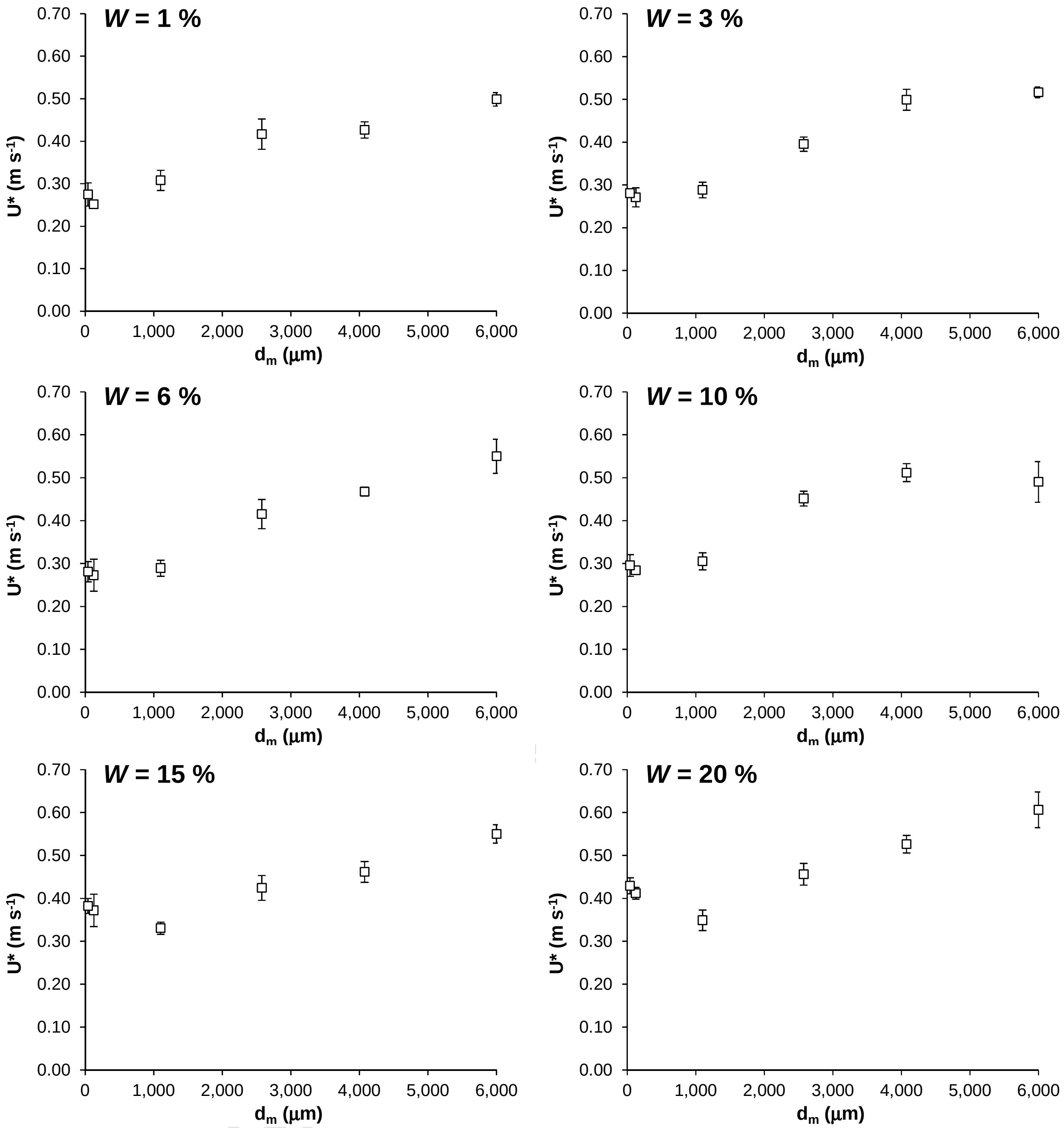

Figure 2. Threshold friction velocities (U^*) regarding particle detachment from the sample centre (moment 3, particles from the sample centre starting to be transported).

3.2. Effect of gravimetric water content

Figure 3 presents the experimental U^* values as a function of W, as well as RSM regression (contour plot) for moment 3. In order to make Figure 3a clearer, standard deviations were omitted and presented as supplementary material (Table S2). The RSM regression presented a good fit, with R^2 = 0.89 (Table 3). In the

ACCEPTED MANUSCRIPT

test for the significance of the regression, the rejection of the null hypothesis (p-value < 0.001) implies that at least one of the independent variables contributed significantly to the model.

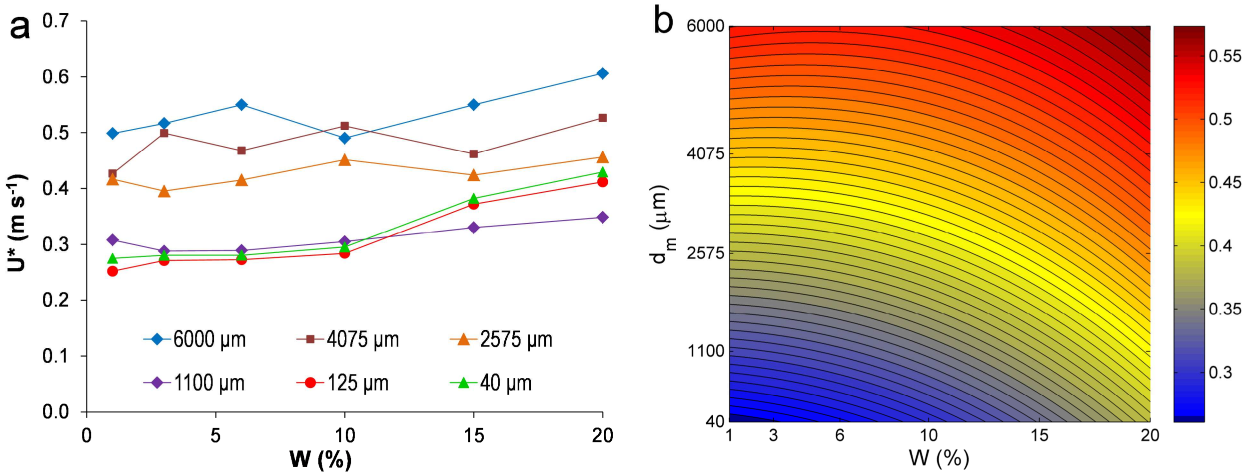

Figure 3. Threshold friction velocities (U^*) as a function of gravimetric water content (*a*) and respective response surface (*b*).

Table 3. Coefficients of the response surface methodology regression and goodness-of-fit.

B_0	B_1	B_2	$B_{1,1}$	$B_{1,2}$	$B_{2,2}$	R^2	**Significance (*p*-value)**
0.4269	0.0438	0.1156	-0.019	0.022	-0.009	0.89	<0.0001

Figure 3a shows that up to 10 % moisture content the experimental U^* values did not change considerably. From 10 % to 20 % moisture content, significant increases were observed for U^*, i.e. 45 % and 25 % for the smallest (d_m of 40 and 125 µm, p-value <0.001) and the largest (d_m = 6,000 µm, p-value <0.001) particles, respectively. This result indicates that erosion of both small and large biochar particles was affected by gravimetric water content, although possibly different mechanisms. The remaining particle size classes tended to maintain similar U^* values, regardless of moisture conditions. However, the response surface applied to the experimental data (Figure 3b), clearly illustrates that the positive effect of moisture content on U^* was more pronounced for small particle size, with an increase of predicted values of U^* from 0.27 to 0.40 m s^{-1}. On the contrary, for coarser particles, the influence of moisture content seemed to be almost negligible, varying between 0.54 and 0.56 m s^{-1}. Indeed, the B_2 coefficient was higher than B_1 (0.12 and 0.04, respectively), which reflects a stronger effect of particle size on predicted U^* rather than moisture content. Although the fitting was very accurate, the model tended to overestimate U^* for particles with d_m = 1,100 µm. In addition it can be argued that the model was heavily weighted towards smaller particle classes (d_m = 40 and 125 µm), which are relatively close in the experimental range and, therefore, a potential source of bias (Myers et al., 2009).

ACCEPTED MANUSCRIPT

These results clearly provided important implications of moisture content in biochar applied in the field. Since the smallest particles are those subjected to eventual erosion episodes, it is important to bear in mind the effect of water content to mitigate their detachment. Therefore, *U** of the smallest particles can be increased by keeping *W* at 15 % or higher.

3.3. Contributions of adhesive and gravity forces

Table 4 presents, for each particle size, the contributions of adhesive (parameter *b* in Eq. (5) and gravity (parameter *a*) forces, calculated using the experimental data for moment 3. The contribution of gravity (*a*) increased with increasing particle size, showing that the weight gain by water absorption by the particles is more relevant to *U** than adhesive forces. The contribution of adhesive forces (*b*) was more pronounced for small particles (d_m of 40 and 125 μm) rather than larger ones, with *b* values for the former (about 8.5×10^{-3}) substantially higher than those for the latter (in the range of 2.4×10^{-3} – 4.4×10^{-3}).

Table 4. Contributions of gravity (*a*) and adhesive forces (*b*) for biochar particle threshold friction velocity (*U**) according to a linear regression model (Eq. (5)).

d_m (μm)	40	125	1,100	2,575	4,075	6,000
a	$2.46{\times}10^{-1}$	$2.32{\times}10^{-1}$	$2.86{\times}10^{-1}$	$4.05{\times}10^{-1}$	$4.55{\times}10^{-1}$	$4.94{\times}10^{-1}$
b	$8.48{\times}10^{-3}$	$8.53{\times}10^{-3}$	$2.82{\times}10^{-3}$	$2.38{\times}10^{-3}$	$2.92{\times}10^{-3}$	$4.45{\times}10^{-3}$
R^2	$8.93{\times}10^{-1}$	$9.16{\times}10^{-1}$	$7.44{\times}10^{-1}$	$5.63{\times}10^{-1}$	$3.32{\times}10^{-1}$	$5.73{\times}10^{-1}$
Significance (p value)	$4.40{\times}10^{-3}$	$2.70{\times}10^{-3}$	$2.70{\times}10^{-2}$	$8.57{\times}10^{-2}$	$2.30{\times}10^{-1}$	$8.12{\times}10^{-2}$

The relatively low R^2 values for the larger particle size classes, dm=2,575 μm and above, are primarily related with the non-linear patterns observed in U* for some of the particle size classes, as can be observed in Figure 3a. The goodness-of-fit of the three smaller particle size classes, with R^2 values between 0.744 and 0.916, with significant and highly significant regressions, are of the same order as those reported by Zhang et al. (2012), R^2 values between 0.689 and 0.810. However, the goodness-of-fit for the three larger particle size classes, R^2 values between 0.573 and 0.332, with non-significant regressions, are lower than those reported by Zhang et al. (2012). A subset of data presenting reduced adhesive effect was selected by excluding the smallest particle size classes (d_m = 40 and 125 μm). This subset for each of the gravimetric water content series was applied to the modified Bagnold model (Zhang et al., 2012; Eq. (6)), by using air density (ρ_{air}) value of 1.2 kg m^{-3} and an average biochar particle density ($\rho_{biochar}$) of 450 kg m^{-3} (Shenbagavalli and Mahimairaja, 2012). Determined values of *A* ranged from 0.09 to 0.13 and, under the best fit (R^2 = 0.87) it equalled 0.12. As shown in Figure 4, by taking *A* = 0.12, the modified Bagnold's model accurately predicted the experimental values of *U** for biochar particles that were not affected by adhesive forces. However, this model underestimated *U** for the smaller particle size classes (d_m of 40 and 125 μm), thereby confirming the results found by (Zhang et al., 2012) for coal particles with mean diameters smaller than 250 μm.

ACCEPTED MANUSCRIPT

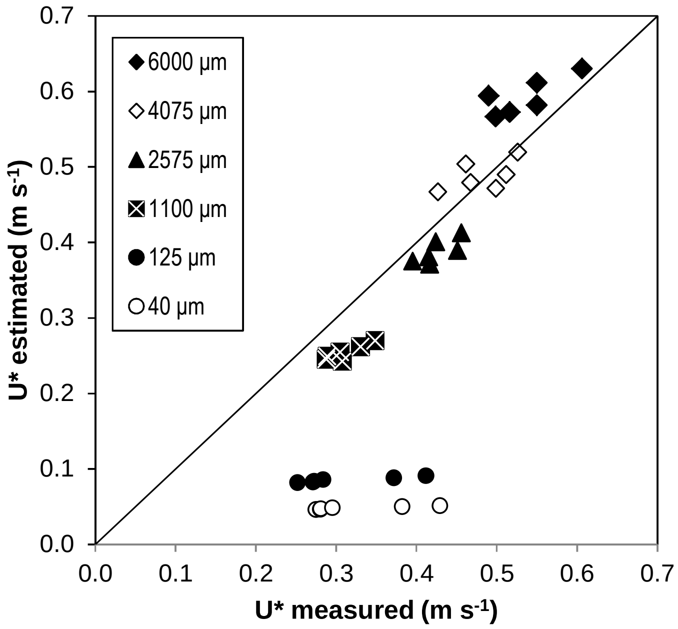

Figure 4. Experimental and calculated U* of biochar particles using Eq. (6)

The modified Bagnold's model can be extended to include the contribution of adhesive forces (see section 2.3). The resulting Eq. (8) was fitted to the complete experimental data set from this study (including the smaller particle sizes classes) in order to estimate c and d, using the previously determined parameter A = 0.12. The goodness-of-fit was lower for $W \geq 15$ % (Table 5), most likely caused by strong adhesive forces at those moisture contents, which increased U* for the smaller particle size classes (as can be seen in Figure 2), thereby decreasing its correlation coefficient. Nevertheless, under the best fit (R^2 = 0.86), c and d were 0.87 and 0.71, respectively. These values were applied to equation 7 to calculate the adhesive effect parameter (β), shown in Figure 5. The calculated β values increased exponentially with decreasing particle size, from 1.7 to 12.9 for W = 1 %, and from 61.2 to 452.5 for W = 20 %.

Table 5. Estimation of c and d coefficients using the modified Bagnold's model (Eq. 8).

***W* (%)**	1	3	6	10	15	20
c	0.87	1.10	1.36	1.80	2.60	3.00
d	0.71	0.70	0.68	0.74	0.87	0.87
R^2	0.87	0.79	0.79	0.80	0.45	0.39

ACCEPTED MANUSCRIPT

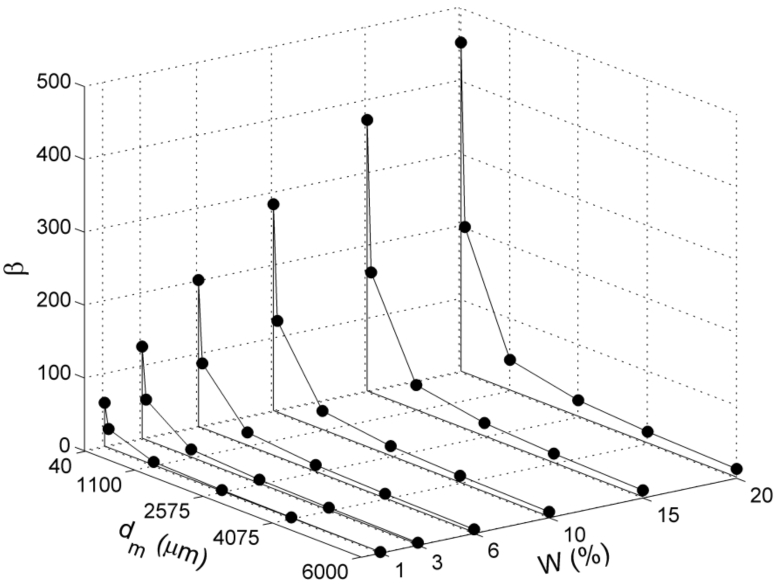

Figure 5. Adhesive effect parameter (β) as a function of gravimetric moisture content and mean particle size (segments between dots provide only a visual connection between calculated β values in the same *W* series).

4. Discussion

In comparison to studies examining the effect of moisture content and particle size on *U** in coal samples, there are some broad similarities, but also important differences. Namely, the studies by Duo-min and Shu-tang (1991) and Zhang et al. (2012) showed similar increases in *U** with increase in particle size. However, the particle size range in the present biochar experiment (<50 µm to >6,000 µm) is much greater than in the referred coal experiments (<45 µm to >1,000 µm), reflecting common differences in particle size distributions of woody biochars and coal. Even at large sizes (>6 cm), biochar particles reached *U** values commonly found for sand particles of 0.4 – 0.5 cm (Fécan et al., 1999). This is most likely explained by the much greater density of sand than biochar, both regarding bulk and particle density. Due to lower inter-particle porosity, sandy soils would be subjected to less air entrainment into the soil. In addition, large biochar particles present a platy morphology compared to spheroidal sand particles, possibly resulting in greater shear stress as air passed over and under the large biochar particles, compared to sand particles. This would suggest that even large biochar particles exposed at the soil surface may also become mobile (by creep or saltation mechanisms) under erosive conditions, i.e. dry bare soil on windy days. However, this study was focused exclusively on the response of biochar particles to controlled varying wind conditions, and additional research on the interaction between soil particles and biochar particles, in wind tunnel simulations and in the field, is needed to provide further quantification.

The effect of moisture content also showed a similar pattern for biochar particles as for coal particles (Duo-min and Shu-tang, 1991; Zhang et al., 2012). The two smaller particle sizes (d_m <125 µm) exhibited increasing adhesive forces with increasing moisture content, with particles ≥1,100 µm experiencing 2-3 times lower adhesive effects than particles ≤ 125 µm. The largest particles size class, >4,000 µm (dm=6,000), appears to show a recurring increase in adhesive effect, although still only approximately half as strong as for the two smaller particle sizes. Possibly, the shape of these largest particles (increased platiness) may have contributed to this effect by increased surface contact. However, the woody feedstock biochar used in this study only had significantly (p-value <0.001) increased U^* values for fine particles at moisture contents of 15 % and 20 %, whereas for coal particles used by Zhang et al. (2012) this appeared to occur at 6 – 8 % moisture content. Possibly, this difference can be explained by the larger porosity of biochar particles, i.e. 55 – 70% (Brewer et al., 2014), compared to coal particles, i.e. 6 – 20 % (Zhang et al., 2012). Therefore, water films on biochar particle surfaces would only develop at greater moisture contents than for coal particles. The modified Bagnold model (Zhang et al., 2012) estimated U^* reasonably well for particles ≤1,100 µm, but markedly worse estimates were found for particles ≥2,575 µm. This implies that, for this type of biochar, the modified Bagnold model may be used with confidence to estimate the wind velocity and biochar moisture content at which particles ≤1,100 µm are likely to become airborne. However, for larger particles the model needs to be developed further.

These findings suggest to only consider moisture contents of 15 % or greater for recommendations (including certifications) regarding storage, transport, and field application of biochar for the purpose of reducing the propensity of particles becoming air-borne. If further increases in U^* can be reached at moisture contents over 20 % requires further research. The smallest particle size considered in this experiment was <50 µm. Many health concerns regarding inhalation of particles focus on respirable suspended particles (<10 µm) or fine particles (<2.5 µm), or even smaller fractions. Although these particle sizes were part of the smallest particle size class used in this study, it is possible that they were undetected. Follow-up experiments with techniques that can detect particles in this size range are required to provide more insight.

Unlike coal, biochar is made from a wide variety of feedstocks, under a range of pyrolysis conditions, resulting in a variety of biochar physical properties. A woody feedstock biochar was used in this study as being representative of many biochars being used in experiments. However, biochar is also produced by pyrolysis of many other feedstocks, such as poultry litter, wastewater sludge, green waste, and biosolids (Jeffery et al., 2011), which are known to differ strongly in particle size distributions, particle morphology and density, (capillary) porosity, etc. (Chia et al., 2015). Therefore, this study's results cannot be directly extrapolated to other biochars, and further studies are urgently needed to fill this knowledge gap and inform policy development. In addition, future studies should also consider effects of saltating particles on threshold friction velocities of biochars, and bench and field studies should consider how soil aggregation and downward movement of fine particles in soils affect biochar erosion by wind.

5. Conclusions

In order to identify interactions between wind and biochar, we conducted a wind tunnel study to determine threshold friction velocities of a woody feedstock biochar for a range of particle sizes and gravimetric moisture contents. For W < 10 %, fine particles (d_m <125 μm) started to erode at U^* as low as 0.27 m s^{-1} whereas large particles (d_m >6,000 μm) eroded at 0.50 – 0.55 m s^{-1}, showing that large biochar particles exposed at the soil surface may also become suspended at threshold friction velocities commonly found for sand particles. However, for $W \geq 15$ %, the moisture content presented greater impacts on smaller than larger particles, by promoting their adhesion and increasing the threshold friction velocity. In turn, larger particles exhibited resistance to erodibility due to weight gain by water absorption. These results provide important implications of biochar moisture content to inform its sustainable development and application. Since smaller particles are more susceptible to detachment in field, avoidance of wind erosion can be achieved by keeping W at 15 % or more to increase safe storage, transport and field application of biochar.

5. Acknowledgements

This work was supported by European Funds through COMPETE and by National Funds through the Portuguese Fundação para a Ciência e a Tecnologia (FCT) within projects PEst-C/MAR/LA0017/2013, EXPLOCHAR (EXPL/AGR-FOR/0549/2013) and CLICURB (EXCL/AAG-MAA/0383/2012), and the post-doctoral grants of J.H. Amorim (SFRH/BPD/48121/2008) and F.G.A. Verheijen (SFRH/BPD/74108/2010).

6. References

Alfaro, S. C., A. Gaudichet, L. Gomes, M. Maillé, 1997. Modeling the size distribution of a soil aerosol produced by sandblasting. J. Geophys. Res, 102, 11239–11249. http://dx.doi.org/10.1029/97JD00403

Andreae, M.O., Merlet, P., 2001. Emission of trace gases and aerosols from biomass burning. Global Biogeochem. Cycles 15, 955-966. http://dx.doi.org/10.1029/2000gb001382

Bagnold, R.A., 1941. The physics of blown sand and desert dunes. London: Methuen.

Blackwell, P., Krull, E., Butler, G., Herbert, A., Solaiman, Z., 2010. Effect of banded biochar on dryland wheat production and fertiliser use in south-western Australia: an agronomic and economic perspective. Soil Research 48, 531-545. http://dx.doi.org/10.1071/SR10014

Borrego, C., Costa, A.M., Amorim, J.H., Santos, P., Sardo, J., Lopes, M., Miranda, A.I., 2007. Air quality impact due to scrap-metal handling on a sea port: A wind tunnel experiment. Atmos. Environ. 41, 6396-6405. http://dx.doi.org/10.1016/j.atmosenv.2007.01.022

Boton, M., Azéma, E., Estrada, N., Radjaï, F., Lizcano, A., 2013. Quasistatic rheology and microstructural description of sheared granular materials composed of platy particles. Physical Review E 87, 032206. http://dx.doi.org/10.1103/PhysRevE.87.032206

Brewer, C.E., Chuang, V.J., Masiello, C.A., Gonnermann, H., Gao, X., Dugan, B., Driver, L.E., Panzacchi, P., Zygourakis, K., Davies, C.A., 2014. New approaches to measuring biochar density and porosity. Biomass Bioenergy 66, 176-185. http://dx.doi.org/10.1016/j.biombioe.2014.03.059

Buchsbaum, L., 2007. Railroads and shippers clash over coal dust. Coal Age 112, 14-15

Chen, W., Zhibao, D., Zhenshan, L., Zuotao, Y., 1996. Wind tunnel test of the influence of moisture on the erodibility of loessial sandy loam soils by wind. J. Arid Environ. 34, 391-402. http://dx.doi.org/10.1006/jare.1996.0119

Chia, C.H., Downie, A., Munroe, P., 2015. Characteristics of Biochar: Physical and Structural Properties, in: Lehmann, J., Joseph, S. (Eds.), Biochar for Environmental Management - Science and Technology Routledge.

Choobari, O.A., Zawar-Reza, P., Sturman, A., 2014. The global distribution of mineral dust and its impacts on the climate system: A review. Atmospheric Research 138, 152-165. http://dx.doi.org/10.1016/j.atmosres.2013.11.007

Cornelis, W.M., Gabriels, D., 2003. The effect of surface moisture on the entrainment of dune sand by wind: an evaluation of selected models. Sedimentology 50, 771-790. http://dx.doi.org/10.1046/j.1365-3091.2003.00577.x

De Capitani, E.M., Algranti, E., Handar, A.M.Z., Altemani, A.M.A., Ferreira, R.G., Barbosa Balthazar, A., Cerqueira, E.M.F.P., Sanae Ota, J., 2007. Wood charcoal and activated carbon dust pneumoconiosis in three workers. Am. J. Ind. Med. 50, 191-196. http://dx.doi.org/10.1002/ajim.20418

Dey, S., 1999. Sediment threshold. Appl. Math. Model. 23, 399-417. http://dx.doi.org/10.1016/S0307-904X(98)10081-1

Dong, Z., Liu, X., Wang, H., Wang, X., 2003. Aeolian sand transport: a wind tunnel model. Sediment. Geol. 161, 71-83. http://dx.doi.org/10.1016/S0037-0738(02)00396-2

Fécan, F., Marticorena, B., Bergametti, G., 1999. Parametrization of the increase of the aeolian erosion threshold wind friction velocity due to soil moisture for arid and semi-arid areas. Ann. Geophys. 17, 149-157. http://dx.doi.org/10.1007/s00585-999-0149-7

Ferreira, A.D., Viegas, D.X., Sousa, A.C.M., 2003. Full-scale measurements for evaluation of coal dust release from train wagons with two different shelter covers. Journal of Wind Engineering and Industrial Aerodynamics 91, 1271-1283. http://dx.doi.org/10.1016/S0167-6105(03)00077-1

Genis A, Vulfson L, Ben-Asher J, 2013. Combating wind erosion of sandy soils and crop damage in the coastal deserts: Wind tunnel experiments. Aeolian Research 9, 69-73. http://dx.doi.org/10.1016/j.aeolia.2012.08.006

ACCEPTED MANUSCRIPT

Han, Q., Qu, J., Zhang, K., Zu, R., Niu, Q., Liao, K., 2009. Wind tunnel investigation of the influence of surface moisture content on the entrainment and erosion of beach sand by wind using sands from tropical humid coastal southern China. Geomorphology 104, 230-237. http://dx.doi.org/10.1016/j.geomorph.2008.08.016

Harrison, R.M., Jones, A.M., Gietl, J., Yin, J., Green, D.C., 2012. Estimation of the contributions of brake dust, tire wear, and resuspension to nonexhaust traffic particles derived from atmospheric measurements. Environ Sci Technol 46, 6523-6529. http://dx.doi.org/10.1021/es300894r

Hashizume, M., Ueda, K., Nishiwaki, Y., Michikawa, T., Onozuka, D., 2010. Health effects of Asian dust events: a review of the literature. Nihon Eiseigaku Zasshi 65, 413-421.

He J-J, Cai Q-G, Tang Z-J, 2008. Wind tunnel experimental study on the effect of PAM on soil wind erosion control. Environ Monit Assess, 145, 185–193. http://dx.doi.org/10.1007/s10661-007-0028-1

IPCC, 2013. Climate Change 2013: The Physical Science Basis. Contribution of Working Group I to the Fifth Assessment Report of the Intergovernmental Panel on Climate Change, in: Stocker, T.F., D. Qin, D., Plattner, G.-K., Tignor, M., Allen, S.K., Boschung, J., Nauels, A., Xia, Y., Bex, V., Midgley, P.M. (Eds.). Cambridge University Press, Cambridge, UK and New York, USA, p. 1535

Ito, A., Penner, J.E., 2005. Historical emissions of carbonaceous aerosols from biomass and fossil fuel burning for the period 1870–2000. Global Biogeochem. Cycles 19, GB2028. http://dx.doi.org/10.1029/2004gb002374

Jacobson, M.Z., 2001. Strong radiative heating due to the mixing state of black carbon in atmospheric aerosols. Nature 409, 695-697. http://www.nature.com/nature/journal/v409/n6821/suppinfo/409695a0_S1.html

Jeffery, S., Verheijen, F.G.A., van der Velde, M., Bastos, A.C., 2011. A quantitative review of the effects of biochar application to soils on crop productivity using meta-analysis. Agric., Ecosyst. Environ. 144, 175-187. http://dx.doi.org/10.1016/j.agee.2011.08.015

Karanasiou, A., Moreno, N., Moreno, T., Viana, M., de Leeuw, F., Querol, X., 2012. Health effects from Sahara dust episodes in Europe: Literature review and research gaps. Environ. Int. 47, 107-114. http://dx.doi.org/10.1016/j.envint.2012.06.012

Lehmann, J., 2007. Bio-energy in the black. Front. Ecol. Environ. 5, 381-387. http://dx.doi.org/10.1890/1540-9295(2007)5[381:bitb]2.0.co;2

Lehmann, J., Gaunt, J., Rondon, M., 2006. Bio-char Sequestration in Terrestrial Ecosystems – A Review. Mitig Adapt Strat Glob Change 11, 395-419. http://dx.doi.org/10.1007/s11027-005-9006-5

Lehmann, J., Joseph, S., 2015. Biochar for Environmental Management: An Introduction in: Lehmann, J., Joseph, S. (Eds.), Biochar for Environmental Management - Science and Technology Routledge.

Lin, D.M., Tsai, S.T., 1991. The relation of the threshold velocity of coal dust to its size and humidity. Appl Math Mech 12, 513-519. http://dx.doi.org/10.1007/bf02015564

Myers, R.H., Montgomery, D.C., Anderson-Cook, C., 2009. Response Surface Methodology: Process and Product Optimization Using Designed Experiments 3rd ed. Wiley, New York.

Nguyen, B.T., Lehmann, J., 2009. Black carbon decomposition under varying water regimes. Org. Geochem. 40, 846-853. http://dx.doi.org/10.1016/j.orggeochem.2009.05.004

Salvi, S.S., Barnes, P.J., 2009. Chronic obstructive pulmonary disease in non-smokers. Lancet 374, 733-743. http://dx.doi.org/10.1016/s0140-6736(09)61303-9

Schmidt, H.P., Abiven, S., Kamman, C., Glaser, B., Bucheli, T., Leifield, J., 2012. Guidelines for biochar production: European biochar certificate version 4.2. Delinat-Institut für Ökologie und Klimafarming, Arbaz (Switzerland)

Shenbagavalli, S., Mahimairaja, S., 2012. Production and characterization of biochar from different biological wastes. International journal of plant, animal and environmental science 1, 197-201

Terzaghi, K., 1996. Soil mechanics in engineering practice. John Wiley & Sons.

Toraño, J.A., Rodriguez, R., Diego, I., Rivas, J.M., Pelegry, A., 2007. Influence of the pile shape on wind erosion CFD emission simulation. Appl. Math. Model. 31, 2487-2502. http://dx.doi.org/10.1016/j.apm.2006.10.012

Verheijen, F., Jeffery, S., Bastos, A., Van der Velde, M., Diafas, I., 2010. Biochar application to soils - A Critical Scientific Review of Effects on Soil Properties, Processes and Functions, Office for the Official Publications of the European Communities, p. 149

Verheijen, F.G.A., Graber, E.R., Ameloot, N., Bastos, A.C., Sohi, S., Knicker, H., 2014. Biochars in soils: new insights and emerging research needs Introduction. Eur. J. Soil Sci. 65, 22-27. http://dx.doi.org/10.1111/ejss.12127

Whitman, T., Nicholson, C.F., Torres, D., Lehmann, J., 2011. Climate Change Impact of Biochar Cook Stoves in Western Kenyan Farm Households: System Dynamics Model Analysis. Environ. Sci. Technol. 45, 3687-3694. http://dx.doi.org/10.1021/es103301k

Zhang, X., Chen, W., Ma, C., Zhan, S., 2012. Modeling the effect of humidity on the threshold friction velocity of coal particles. Atmos. Environ. 56, 154-160. http://dx.doi.org/10.1016/j.atmosenv.2012.04.015

Zhang, X., Chen, W., Ma, C., Zhan, S., 2013. Modeling particulate matter emissions during mineral loading process under weak wind simulation. Science Total Environment 449, 168-173. http://dx.doi.org/10.1016/j.scitotenv.2013. 01.050

ACCEPTED MANUSCRIPT

Highlights

• Wind erosion of biochar was assessed through wind tunnel simulations

• Moisture content lower than 10 % does not prevent erosion of fine particles

• Higher moisture increases adhesion of fine particles and weight of large particles

• Minimum 15 % moisture is recommended for reducing wind erosion of biochar

ACCEPTED MANUSCRIPT